Development of Silicon Pad Detectors and Readout Electronics for a Compton Camera

A. Studen [a,*] V. Cindro [a] N. H. Clinthorne [b] A. Czermak [c]
W. Dulinski [d] J. Fuster [e] L. Han [f] P. Jalocha [c] M. Kowal [c]
T. Kragh [f] C. Lacasta [e] G. Llosá [e] D. Meier [b] M. Mikuž [a]
E. Nygård [g] S. J. Park [f] S. Roe [h] W. L. Rogers [b] B. Sowicki [c]
P. Weilhammer [h] S. J. Wilderman [f] K. Yoshioka [g] L. Zhang [f]

[a] *Institute Jožef Stefan and Department of Physics, University of Ljubljana, Ljubljana, Slovenia*

[b] *Medical School, University of Michigan, Ann Arbor, U. S. A.*

[c] *Niewodniczanski Institute of Nuclear Physics, Crakow, Poland*

[d] *LEPSI, IN2P3/CNRS-ULP, Strasbourg, France*

[e] *Inst. de Fisica Corpuscular, CSIC, Universitat de Valencia, Valencia, Spain*

[f] *College of Engineering, University of Michigan, Ann Arbor, U. S. A.*

[g] *Ideas ASA, Oslo, Norway*

[h] *CERN, Geneva, Switzerland*

Abstract

Applications in nuclear medicine and bio-medical engineering may profit using a Compton camera for imaging distributions of radio-isotope labelled tracers in organs and tissues. These applications require detection of photons using thick position-sensitive silicon sensors with the highest possible energy and good spatial resolution. In this paper, research and development on silicon pad sensors and associated read-out electronics for a Compton camera are presented. First results with low-noise, self-triggering VATAGP ASIC's are reported. The measured energy resolution was 1.1 keV FWHM at room temperature for the ^{241}Am photo-peak at 59.5 keV.

* Corresponding author
Email address: Andrej.Studen@ijs.si (A. Studen).

1 Introduction

A Compton camera collimates gamma(γ)-rays using a first detector where γ-rays Compton scatter and a second detector where γ-rays are measured by photo-absorption [1]. Both detectors measure in coincidence and each coincidence event allows one to reconstruct a cone [Fig. 1]. The tip of the cone is measured from the position of the Compton interaction in the first detector. Together with the position measured in the second detector one derives the axis of the cone. The opening angle of the cone with respect to its axis, θ, is derived from the energy, E_e in the first detector, and $E'_\gamma = E_\gamma - E_e$ in the second detector, using the relation $\sin(\theta/2) = \sqrt{m_e c^2 E_e / 2E_\gamma(E_\gamma - E_e)}$, where $m_e c^2 = 511$ keV.

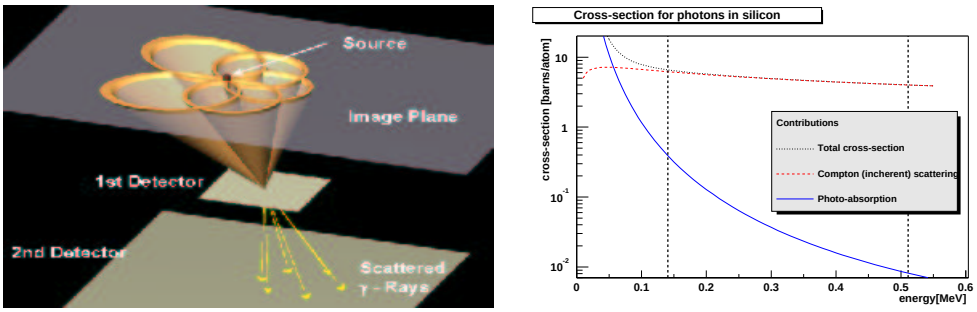

Figure 1. Left: schematic drawing of the first and the second detector in a Compton camera [2]. The coincident measurements in both detectors allow one to derive cones which intersect at the gamma source in the image plane. Right: cross-sections for photo-absorption and Compton scattering in silicon as a function of energy from 0 to 550 keV.

The first detector is produced from silicon (atomic number $Z = 14$, atomic mass $A = 28$), which is a good Compton scatterer- and an ideal detector material. Fig. 1 shows the cross-sections for photo-absorption and Compton scattering in silicon as a function of energy, E_γ, from 0 to 550 keV. One can see that the cross-section, σ_c, for Compton interaction is much larger than for photo-absorption and that the ratio of the Compton to total interaction is 94 % at 140 keV and 99.7 % at 511 keV. The probability for Compton interaction is given by $p_c = 1 - \exp[-\varrho d\sigma_c(E_\gamma)]$, where $\varrho \approx 4.2 \times 10^{22}$ atoms per cm^3. For silicon thickness of $d = 1$ mm one derives $p_c(511\text{ keV}) \approx 2.0$ %. The probability for Compton scattering dominates over photo-absorption in the range of energies used in medical imaging (140 keV for ^{99m}Tc to 511 keV for positron emitters.). The total amount of silicon for the scatter detector has to be optimized for single Compton interactions. For 511 keV photons the optimal thickness is near 16 mm. The second detector can be a "high Z" scintillator like NaI, as used in C-SPRINT, a Compton camera prototype [3].

2.1 Silicon Pad Sensors

Various geometries of silicon pad sensors were designed [4,5] and processed by SINTEF [6] and CSEM [7]. Fig. 2 illustrates the design of the silicon pads used.

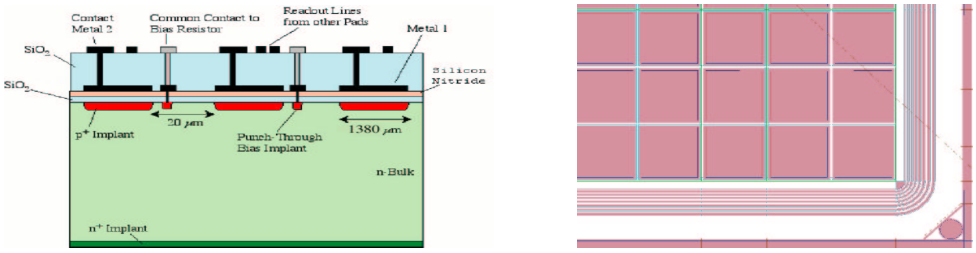

Figure 2. Left: Cross-sectional view of an AC coupled silicon sensor showing silicon bulk, implants and metal layers. The bulk thicknesses in the range from 0.3 mm to 1 mm were processed. Right: top view of a corner showing metal 1 layer of pads and guard rings. The pad size is 1.4×1.4 mm^2.

The sensors are p-in-n doped with a double metal layer. Metal-1 fully covers the pads, metal-2 routes lines from the pads to the sensor side. The two metal layers are separated by SiO_2 (CSEM) or polyimide (SINTEF). Sensors from CSEM are AC coupled and punch-through biased, sensors from SINTEF are DC coupled. The pad size is 1.4×1.4 mm^2 which allows one to measure the tip of the cone with a precision of 1.4 mm FWHM. The main contributions to electronic noise in a readout channel are the current into the pre-amplifier and the capacitive load at the pre-amplifier input. Fig. 3 (left) shows the leakage current and backplane capacitance in a single pad of a 1 mm thick sensor as a function of its backplane voltage from 0 to 500 V. From the capacitance measurement we infer a full depletion voltage of $U_{\mathrm{FD}} = 320$ V. The leakage current at 320 V is 200 pA per pad. Fig. 3 (right) shows the square of the count rate of the photo-absorbed photons from ^{241}Am in 25 silicon pads as a function of the backplane voltage. The count rate increases as the square root of the backplane voltage and saturates for voltages above full depletion of 320 V, which agrees with the result obtained in the capacitance measurement. Silicon sensors are mainly sensitive in the depleted region where the electric field separates electron-hole pairs. For the count rate measurement all 25 pads were read out by the VATAGP [8], and the counting threshold was just below the photo-absorption peak. $U_{\mathrm{FD}} = 320$ V for a 1 mm thick silicon sensor indicates a bulk resistivity, $\rho = d^2/2\mu_{\mathrm{n}}\varepsilon\varepsilon_0 U_{\mathrm{FD}} \approx 10$ kΩcm, where $1/2\mu_{\mathrm{n}}\varepsilon\varepsilon_0 = 31.5$ kΩcm $\times$ 100 V/mm^2.

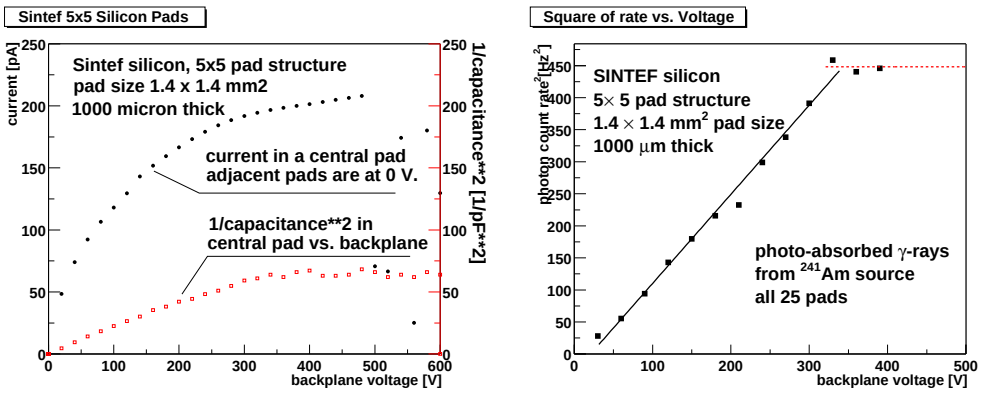

Figure 3. Measurements in a 1 mm thick silicon detector, processed by SINTEF. Left: leakage current and pad-to-backplane capacitance vs. backplane voltage. Right: count rate of photo-absorbed photons from ^{241}Am in silicon vs. backplane voltage.

2.2 Charge Sensitive Readout and Triggering

The energy of Compton electrons deposited in a silicon sensor ranges from 0 keV to the "Compton edge" at $E_{\max} = 2E_\gamma^2/(m_e c^2 + 2E_\gamma) \approx 340$ keV for $E_\gamma = 511$ keV and generates 0 to ≈ 95000 eh-pairs which are measured by charge sensitive amplifiers (CSA). The readout chip used here, the VATAGP, contains 128 CSAs and "slow" shapers (VA-part) with sample-and-hold and a multiplexer for sequential readout [Fig. 4]. The VATAGP also contains 128

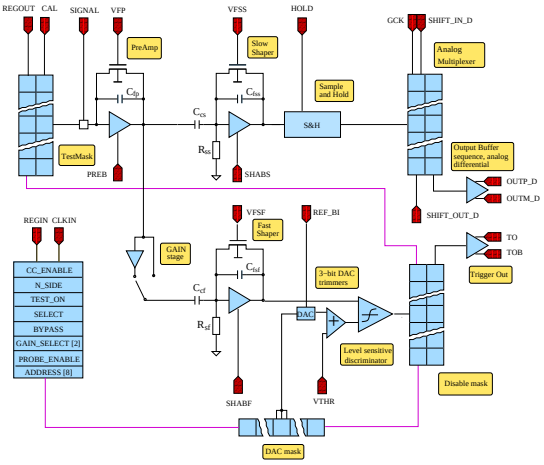

Figure 4. Schematic diagram of one of 128 channels of the VATAGP.

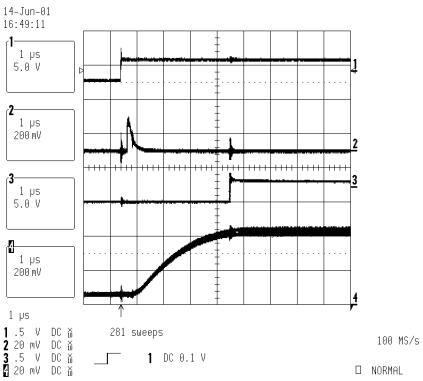

Figure 5. Screenshot from the oscilloscope showing 4 signals measured on the VATAGP: Voltage step for charge injection (line 1) causes a trigger on TO (line 2). After 4 μs delay the HOLD (line 3) is activated to sample and hold the analog outputs from all channels (a single channel is shown on line 4).

"fast" shapers (TA-part) followed by discriminators. The discriminator thresh-

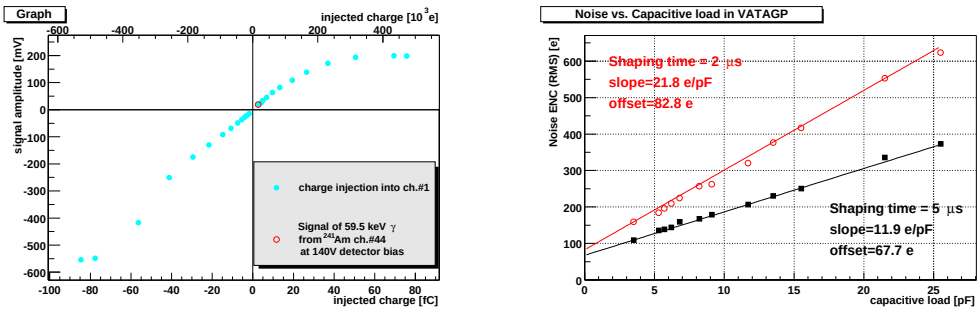

Figure 6. Measurements from the VA part in the VATAGP. Left: dynamic range measured by charge injection into one channel. Right: noise vs. capacitive load measured at a shaping time of 2 μs and 5 μs.

old can be adjusted for all channels in common, the threshold offsets can be adjusted individually for each channel using 3 bit DACs. The "fast" shaper has a signal peaking time of 200 ns and is used to trigger the sampling of the "slow" shaped signal at its peak, where the peaking time of the "slow" shaper can be adjusted between 2 μs and 6 μs. Fig. 5 illustrates charge injection into one pre-amplifier, the triggering, generation of the hold and sampling of the "slow" shaped signal. Fig. 6 (left) shows the dynamic range in the VA-part of the VATAGP measured by charge injection into one channel. The response is linear in the range from -200 000 e to +100 000 e corresponding to -720 keV to +360 keV which allows one to measure signals up to the Compton edge. Fig. 6 (right) shows the electronic noise in a single CSA versus the capacitive load measured at 2 μs and 5 μs peaking time. The linear fit to the data gives respectively 83 e + 22e/pF and 68 e + 12e/pF *rms* noise. If several channels are read out one usually removes common-mode in each event which may reduce the noise. The VATAGP allows one to adjust the control currents and voltages individually or to apply one main control (MBIAS) from which all other controls are derived internally. The noise measurements were performed with VA controls adjusted for low noise.

2.3 Energy Spectra Measured in Silicon Pads with VATAGP

The silicon pads (of a single metal layer sensor) were directly wire-bonded to inputs of the VATAGP in order to measure the energy spectra from γ-sources. Fig. 7 (left) shows two energy spectra from ^{241}Am and ^{57}Co measured in a single channel of a 500 μm thick sensor acquired by an oscilloscope. One can see the photo-peaks for ^{241}Am at 59.5 keV and for ^{57}Co at 122 keV and 136 keV. The peaks were fit by Gaussian functions giving energy resolution of 1.1 and 1.2 keV FWHM. These spectra were measured with VA controls adjusted for low noise. Fig. 7 (right) shows the energy spectrum of ^{241}Am measured in all 25 channels of a 1 mm thick sensor, acquired by the VA-DAQ, where readout was triggered by the TA-part of the VATAGP. For this measurement MBIAS

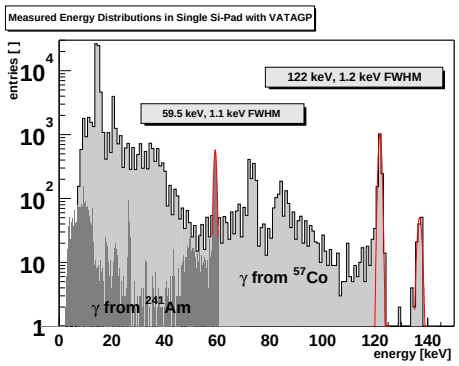

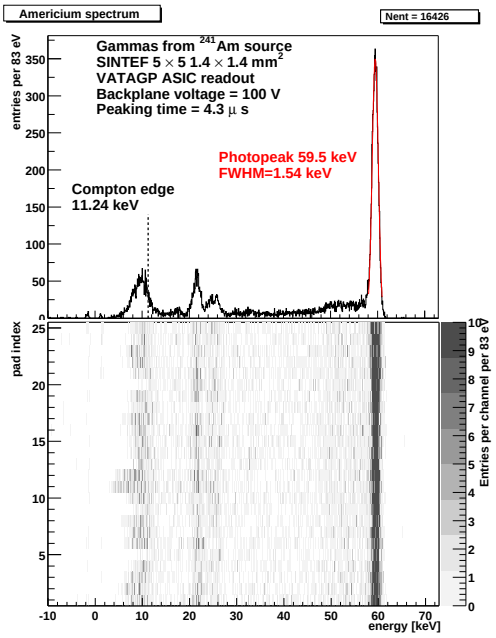

Figure 7. Energy spectra from γ-sources measured in 5×5 silicon pad sensors with VATAGP readout. Above: measurement from a single pad acquired by an oscilloscope. Right: measurement in 25 pads acquired by VA-DAQ [9].

was set at its nominal value and all controls were derived internally on the VATAGP. The spectrum shows the photo-peak of ^{241}Am in all pads aligned at 59.5 keV with an energy resolution 1.5 keV FWHM. One can also see a photo-peak at 26.3 keV from ^{241}Am, the Ag X-ray lines at 22.16 keV and 24.94 keV and entries near the Compton edge at 11.24 keV. The silicon sensor aims for an energy resolution of about 1 keV FWHM, corresponding to an angular resolution of $\approx 2.5^\circ$ FWHM for ^{99m}Tc at 40° scattering angle, which is comparable to contributions from Doppler broadening ($\approx 4^\circ$ FWHM for ^{99m}Tc at 40° scattering angle).

3 Applications: High Resolution PET and Compton Probe

Fig. 8 (left) shows a schematic drawing of a positron emission tomograph (PET) for imaging small animals (*i.e.* mice) [10]. The bio-medical research (neurology, oncology, genetics) on small animals demands sub-millimeter spatial resolution. Position sensitive silicon sensors "S" inside a conventional scintillator "P" measure the position of the Compton scatters near the object. The main three types of events, charaterized by interactions of the two 511 keV photons, are: "S&S", "S&P" and "P&P". With (500 μm)^3 segmentation in "S" one may achieve at the center of the tomograph a precision of 500 μm/$\sqrt{2}$ $\approx$ 350 μm for "S&S" events. The (inherent) limits for spatial resolution are of course the positron range (cusp-shaped distribution with 200 μm FWHM for ^{18}F positrons) and the acollinearity of the annihilaton photons ($\approx 0.25^\circ$ FWHM). Fig. 8 (right) shows a drawing of a Compton probe

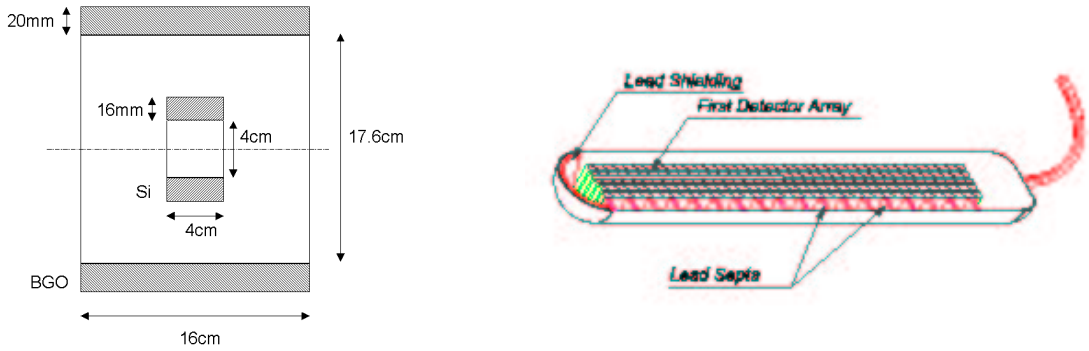

Figure 8. Applications using Compton scattering in silicon. Left: Schematic drawing of a very high resolution PET for imaging small animals with segmented silicon sensor inside and scintillators with photo-multiplier (not shown) outside [10]. Right: drawing of a Compton probe for imaging the prostate [11]. A stack of segmented silicon sensors is mounted inside a cylindrical housing.

for imaging the prostate [11]. The probe is aimed at screening of prostate cancer, the second most common cancer diagnosed in males. The probe could be inserted intra-rectal, close to the prostate, improving position resolution and reducing background from more distant organs. The probe will work in coincidence with a secondary scintillation detector positioned outside the patient.

4 Summary

Research and development on silicon pad sensors and associated readout electronics for a Compton camera was presented. Silicon is a good scatter and an ideal detector material in the energy range used in nuclear medicine. Silicon pad sensored processed by SINTEF show very low leakage currents of 200 pA per pad. Using the 128 channel VATAGP readout chip we measure an energy resolution of 1.1 keV FWHM at 59.5 keV ^{241}Am photo-peak and 1.2 keV FWHM at 122 keV ^{57}Co photo-peak. The dynamic range and the noise of the VATAGP were characterized with the goal of using this chip or one of its succesors in applications like small animal PET or Compton probe.

References

[1] R.W. Todd *et al.* "A Proposed gamma-Camera". *Nature*, **251** (1974) 132.

[2] J.W. Le Blanc. *"Compton Camera for Low Energy Gamma-ray Imaging in Nuclear Medicine Applications"*. PhD thesis, University of Michigan, (1999).

[3] J.W. LeBlanc. "C-SPRINT: A Prototype Compton Camera System for low Energy Gamma Ray Imaging". *IEEE, Trans. Nucl. Sci.*, **45** (1998) 3.

[4] P. Weilhammer *et al.* "Si Pad Detectors". *Nucl. Instr. Meth.*, **383** (1996) 89-97.

[5] D. Meier *et al.* "Silicon Detector for a Compton Camera in Nuclear Medical Imaging". *submitted to Trans. Nucl. Sci.*, Preprint at CERN-EP/2001-009.

[6] SINTEF. Foundation of Scientific and Industrial Research at the Norwegian Institute of Technology, Electronics and Cybernetics, Microsystems. http://www.oslo.sintef.no/ecy/. Oslo and Trondheim, Norway.

[7] CSEM. Centre Suisse d'Electronique et de Microtechnique SA. Rue Jaquet-Droz 1, P.O. Box 41, CH-2007 Neuchtel, Switzerland.

[8] Integrated Detector and Electronics (Ideas ASA). http://www.ideas.no. Pb.315, Veritasveien 9, N-1322 Høvik, Norway, Tel: ++47-6755-1818.

[9] B.M. Sundal. *"Construction and Development of Readout Systems for Radiation Detection"*. PhD thesis, University of Oslo, Dep. of Physics, (1999).

[10] S.J. Park, L. Han, and *et all* S.J. Wilderman. "Experimental Setup for a Very High Resolution Animal PET Based on Solid-state Detector". Conference Record 2001 IEEE Nucl. Sci. Symp. and Med. Imag. Conf., San Diego, Nov 4-10 (2001).

[11] L. Zhang. "An Innovative High Efficiency and High Resolution Probe for Prostate Imaging". *Journal of Nuclear Medicine*, **41** (2001) 4, Suppl.